



Coastal retreat and sea-cliff dynamic on the North Atlantic coast (Gerra Beach, Cantabrian Coast, Spain)

Enrique Serrano¹ · José Juan de Sanjosé² · Manuel Gómez-Lende³ · Manuel Sánchez-Fernández² · Alvaro Gómez-Gutiérrez²

Received: 4 September 2022 / Accepted: 22 December 2023 / Published online: 20 January 2024
© The Author(s) 2024

Abstract

Gerra is small beach located at the foot of a cliff on the Western coast of Cantabria (North of Iberian Peninsula). It has a sandy distal part and a proximal part at the foot of the cliff made up of boulders, supported by rockfalls and landslides from the cliff. Claystones, limestones and marls of the Triassic and Cretaceous ages form the cliff. To study geomorphological processes, a geomorphological map was drawn up; analysis of the beach deposits as texture, granulometry and Atterberg limits; analysis of photogrammetric flights between 1957 and 2017; drone flights between 2017 and 2020; and geomatic monitoring of the cliff and the beach by means of a terrestrial laser scanner (TLS) between 2012 and 2019. The processes involved in the coastal dynamic and retreat of the cliff and beach have been established, as well as the rates of erosion and retreat, which coincide with other beaches on the Cantabrian Coast. The current dynamics are characterized by the moderate regression of the coastline and greater regression and dynamism at the cliff-top, which implies the gradual degradation of the cliff due to loss of verticality. Among the factors involved in the cliff degradation, the main changes in the present and future evolution of the sea cliff can only be ascribed to sea level rise.

Keywords Coastal geomorphology · Beaches · Cliffs · Geomatic techniques · UAV

Introduction

Coastal changes are highly problematic to coastal engineering as they can affect infrastructures and buildings. On the cliffs, both natural changes such as large wind and storm-wave events and sea level rise and man-induced changes such as large-scale coastal engineering works lead to larger and swifter spatial and temporal changes, and they affect inhabited areas causing damage to private property through cliff failure. This is of great relevance to public authorities because such events present a great threat to the safety of residential areas and infrastructures along the cliff. All processes involved in and causes of such swift changes to cliff stability must be understood and studied in detail so as to provide the relevant authorities with data-driven spatial-temporal models of cliff erosion (Young and Ashford 2008; Kuhn and Prüfer 2014; Letortu et al. 2015a). Concern for the shoreline response to climate change is raised because it is seen as a real threat to natural and human habitats (Nicholls et al. 2007; Burden et al. 2020).

Local cliff morphology and retreat rates reflect the balance between marine action and subaerial erosion through

✉ Enrique Serrano
e.serrano@uva.es

José Juan de Sanjosé
jjblasco@unex.es

Manuel Gómez-Lende
manuel.gomezlende@unican.es

Manuel Sánchez-Fernández
msf@unex.es

Alvaro Gómez-Gutiérrez
alvgo@unex.es

¹ Department of Geography, Pangea Research Group, University of Valladolid, Plaza del Campus s/n, 47011 Valladolid, Spain

² INTERRA Research Institute for Sustainable Territorial Development, University of Extremadura, Avenida de la Universidad s/n, 10003 Cáceres, Spain

³ Department of Geography, University of Cantabria, Avenida de Los Castros 44, 39005 Santander, Spain

a wide variety of factors, as tidal range, wave regime, rock strength, lithology and climate, taking place on different scales and rates. All these factors and processes, such as mass movements, seepage and surface runoff erosion, generate long-term coastal cliff erosion, though their relative contributions are variable both in time and space (Brunsden 2002; Brunsden and Lee 2004; Naylor et al. 2010; Kuhn and Prüfer 2014; Letortu et al. 2014, 2015b; Trenhaile 2016).

Geomatic techniques have been used frequently and provide a useful tool for coastal and dynamic studies, but technical advances have now led to greater accuracy. The analysis of historical aerial photographs, topographic maps and survey plans covering several decades have been the most common methodologies for observing cliff changes. Measurements of retreat rates taken on the cliff top provide incomplete information since the data accuracy of aerial images is metric or decimetric and the only line of view is vertical (Kuhn and Prüfer 2014; Letortu et al. 2015a). The application of terrestrial laser scanner TLS opens up new possibilities deriving from greater spatial resolution and accuracy and the higher frequency of geomatic surveys. The use of the Terrestrial Laser Scanner (TLS) technique to monitor processes on the cliff top, walls, talus and beaches is leading to considerable advances in the knowledge of coastal dynamics (Benumof and Griggs 1999; Rosser et al. 2005; Young and Ashford 2006; Marques 2006; Pierre and Lahousse 2006; Dornbusch et al. 2008; Olsen et al. 2009; Young et al. 2009;

Kuhn and Prüfer 2014; Letortu et al. 2015b; Sanjosé et al. 2018). Recently, unmanned aerial vehicles (UAV) and photogrammetry have allowed coastal Cliff monitoring at detailed spatio-temporal scale (e.g. Gómez-Gutiérrez and Goncalves 2020).

Coastline and sea cliff retreat along the Cantabrian Coast, the Northern coast of the Iberian Peninsula aligned from East to West (Fig. 1), have been monitored and major changes on the beaches detected (Losada et al. 1991; Garrote et al. 2001, 2002; Lorenzo et al. 2007; Flor-Blanco et al. 2015; Sanjosé et al. 2016, 2018).

The aim of this work is to analyze the structural and geomorphological characteristics of a coastal area based on pre-existing knowledge of the cliff degradation retreat over the last 60 years. Geomorphic processes on the cliff, such as landslides, were tracked by means of geomatic techniques (aerial photogrammetry, Light Detection and Ranging—LIDAR, UAV and TLS). This is the first step towards improving our knowledge of the processes and landforms involved in the retreat and it is planned to include broader areas of the coast in coming works. This research is part of a long-term monitoring program of the Cantabrian Coast aimed at quantifying geomorphic behaviour, local retreat rates and understanding the coastal dynamic in the local anthropogenic and climate change contexts. The final aim is to provide useful information on processes, risk and threats to the coastal area and to provide local planning authorities with practical information.

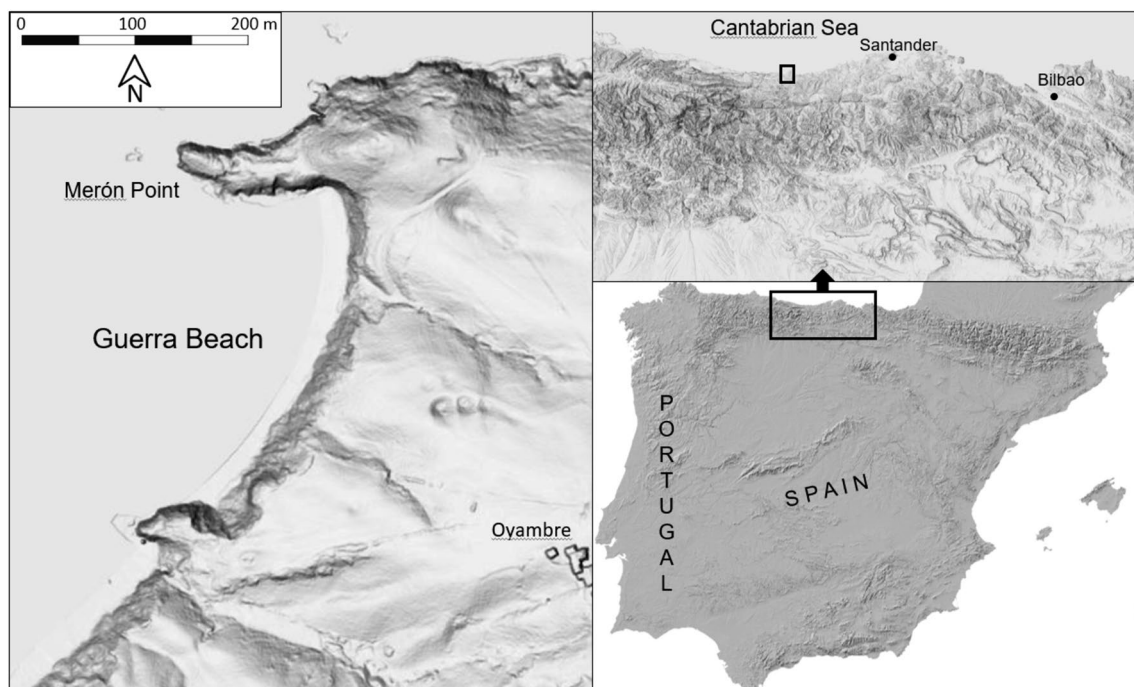


Fig. 1 Location of the Gerra Beach

The study area

The Gerra Beach ($43^{\circ} 24' 03''$ N; $4^{\circ} 21' 18''$ W) is located on the Cantabrian coast (Northern Spain) in the Bay of Biscay (Atlantic Ocean) and the beach is the Eastern area of the San Vicente-Merón beach system, located 700 m NW of the village of Gerra (Fig. 1). The Cantabrian Coast includes a broad typology of sea cliff and low coast (beaches, marshes, estuaries), where marine and human actions have produced considerable changes (Rivas and Cendrero 1994; Bruschi and Remondo 2019; Flor-Blanco et al. 2022). 77% of the Cantabrian Coast is formed by steep cliffs averaging between 20 and 70 m in height. The remaining 23% are embayed beaches, estuaries and aeolian dune fields with a meso-tidal range. The climate is temperate maritime with average winter temperatures of around $14\text{--}15^{\circ}\text{C}$ and annual rainfall ca. 1000–1200 mm. It is an important site for surfers and swimmers with an access to the Gerra Beach by a dirt track, but human influence is restricted to a minimum and the cliffs are undefended.

The geology of the studied area is characterized by two main structures, the syncline flank with the strata dipping to the South and faulted, and a diapiric structure on the edge of the cliff (Fig. 2). The East side is composed of Upper Eocene sandstones, conglomerates and pinky limestone, and Upper Eocene–Oligocene marls, limestone, sandstone (turbiditic facies) and breccias. The West side is composed of Triassic claystone, gypsum and salts (Fig. 2). The diapiric structure implies greater lithostratigraphic complexity, added to Tertiary tectonics leading to folding and thrusting of the whole sequence to the Southeast (Heredia et al. 1990; IGME 2009). Structural control resulted in folded layers comprising a wide variety of geotechnical competencies, from hard limestone to very soft claystone.

The Gerra and San Vicente-Merón beach system stretches to 3 km and three old flat erosional surfaces, locally named “rasas”, can be distinguished at 40–60 m, 65–75 m, and 5–6 m height (Hernández-Pacheco and Asensio-Amor 1966; Moñino 1987; González-Amuchástegui et al. 2005; Domínguez-Cuesta et al. 2015). Hernández-Pacheco and Asensio-Amor (1966) described the depositional sequences made up of basal gravels with clays and aeolian sands on the top, related to sea level changes. The upper level was dated as preglacial ($71,570 \pm 13,400$ yr BP, Garzón-Heydt et al. 1996). According to the bibliography these landforms can be considered as old marine planation surfaces or marine terraces (Hernández-Pacheco and Asensio-Amor 1966; Flor 1983; Moñino 1987; Flor and Flor-Blanco 2014; Domínguez-Cuesta et al. 2015; Flor-Blanco et al. 2022). The Gerra Beach is located in a small cove of 350 m length protected by the Merón Point.

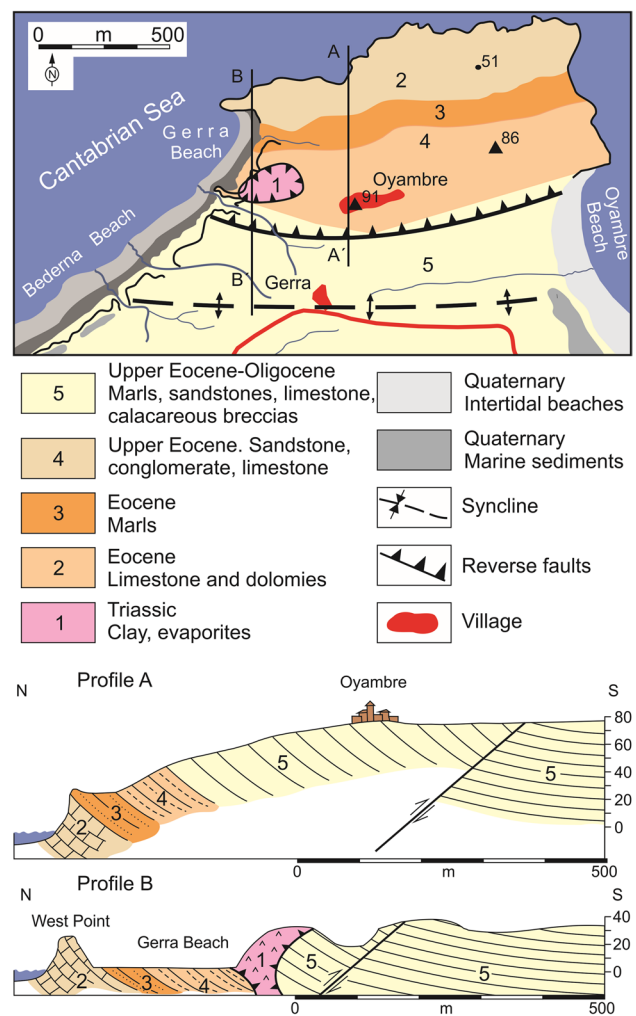


Fig. 2 Geological sketch and profiles of the Gerra area (From IGME 1990, 2009)

The Gerra system is shaped by a beach and a cliff topped by the old flat erosional surface at 40–60 m high, degraded by karst and fluvial processes. The cliff-face is approximately 40 m in height.

In the intertidal zone at the foot of the cliff a boulder beach of rounded cobbles, pebbles and boulders has been developed. The clasts are supplied by erosion on the cliff, where the claystone outcrops show concave profiles. Slope instabilities located on the cliff, ranging in magnitude with volumes of several thousand cubic meters, have recently affected the cliff-top settlements of the El Puntal neighborhood, three kilometers to the West of Gerra beach.

The 80% of the prevalent littoral drift currents along the San Vicente-Merón beaches in open water is from the NW, with other main components come from the W, N, and NE. The dominant wind directions also came mainly from the W–NW direction (30%) although the wind drift shows a wide variability (Garzón-Heydt et al. 1996;

González-Amuchástegui et al. 2005; Garrote et al. 2018). The studied area of the Cantabrian Coast has mesotidal character with the mean tidal range of 2.8 and the maximum values around 5 m at high tide. The wave system is characterized by wave height (Hs) values around 2 m and a recorded maximum historical data (1958–2018) close to 12 m. The historical record of Hs data only shows six times with a maximum monthly higher than 8 m, and five of them occurred after 2007 (Garrote et al. 2018; Sanjosé et al. 2018; Rasilla et al. 2018; Bruschi and Remondo 2019).

Coastline and sea-cliff retreat have been observed along the Cantabrian Coast and major changes on its beaches have been detected (Losada et al. 1991; Garrote et al. 2001, 2002; Lorenzo et al. 2007; Flor-Blanco et al. 2015, 2022; Sanjosé et al. 2016, 2018, 2020). Storms have played an important role in its geomorphological evolution, producing considerable changes in sandy coasts linked to storm events (Sanjosé et al. 2018; Flor-Blanco et al. 2021). No significant temporal trends have been observed in storms along the Northern coast of Spain between 1948 and 2018 except for increased storm activity between the 1960s and 1980s, which reached a maximum around the 1980s and diminished from the 1990s (Rasilla et al. 2018). There were some exceptional events, such as the longest and most intense sequence of storms during the winter of 2013–2014 (Sanjosé et al. 2016, 2018; Garmendia et al. 2017).

Methodology

Geomorphology, deposits, rocks analysis and UAV

A geomorphological map based on the slope and coastal processes was drawn up using remote sensing tools (UAV DEM), geomatic data and fieldwork. The map represents eighteen landforms of cliff and beach units, focusing mainly on active landforms and processes. Brunsten (2002) pointed out the importance of geomorphology for research into slope stability and coastal cliffs and the usefulness of the geomorphological map to detect previous processes and landforms involved in the changes, deformations and dynamics of cliff and rocky coast.

The fieldwork was based on five sedimentary profile surveys from the cliff to the sea along the beach. Particle morphology and grain size facilitate knowledge of the main processes involved in sediment transport at the cliff foot and on the beach. Analysis has been made of beach sediments by plots along the five profiles taking four samples at each profile. The “A” axe size, fabric, clast roundness and clast sphericity of clasts were measured on the field on grids including 100 clasts (Folk 1980; Tucker 1988). Fines sediments were analyzed in the laboratory. After preparation, the samples were sieved by wet shaker sieve method, with

a whole-grade interval with 10 mesh and sizes between 4 and 0.0625 mm (Folk 1980, p. 23), and then their texture parameters were measured (Tucker 1988, 2001; Simon and Kenneth 2001; Blott and Pye 2001). The coarse grain sizes, pebbles, cobbles and boulders were classified according to the Udden-Wentworth scale. In the clays and sands below the cliff, the Attemberg Limits (Liquid and Plastic) were estimated to know the origin and behaviour of sediments by means of the Plasticity and Liquidity indices (Das 2006).

In order to complete the cartography an UAV flight was carried out in November 2018 using a fixed-wing Ebee Classic (senseFly) fitted with a calibrated camera, a Sony WX 220 RGB with a sensor of 6.16 × 4.63 mm, resolution of 18.2 Mp and focal length of 4.57 mm. The flight obtained 173 images at a height of 100 m a.s.l., supported by 20 on-land control points surveyed using a GPS-RTK (GNSS Leica 1200). The flight of the UAV supplied a point cloud of 68 million points. Following the corrections of the IGN real-time positioning service, a mean-square planimetric/altimetric RMSE_{x,y,z} error of ± 20 mm was obtained. The dataset was processed using the photogrammetric software Pix4D mapper Pro, obtaining Root Mean Square Errors in georeferencing and scaling of 4.2, 2.9 and 3.6 cm for the X, Y and Z coordinates respectively. From the Digital Elevation Models (DEM) contour lines with maximum errors of ± 4 cm, an orthophotograph was obtained and the geomorphological map drawn up.

Analysis of sea storms (1985–2020)

Sea storms in the Cantabrian Coast were inventoried from the State Meteorological Agency data, available since 1985, and using the daily swell data from 1985 to 2000. These data were checked against the statistical data of swells recorded by REDCOS (Coastal Network of Swells at State Ports), which coincided in all cases. Days with waves of between 5–6 m and over 6 m were selected (Table 1). In Somo Beach,

Table 1 Number of days by years with large waves in the Cantabrian Coast

| Years | Swell height | | | |
|-----------|--------------|--------|-------|--------|
| | 5–6 m | | > 6 m | |
| | Days | Storms | Days | Storms |
| 1985–1989 | 2 | 2 | 0 | – |
| 1990–1994 | 2 | 2 | 0 | – |
| 1995–1999 | 9 | 8 | 3 | 2 |
| 2000–2004 | 2 | 2 | 2 | 2 |
| 2005–2009 | 3 | 2 | 3 | 2 |
| 2010–2014 | 4 | 3 | 6 | 3 |
| 2015–2017 | 0 | – | 0 | – |
| 2019–2020 | 11 | 3 | 4 | 3 |

50 km to the West of the Gerra Beach, the coincidence between large swells and high tides only it is significant on the retreat of the shoreline if it coincides in time (Sanjosé et al. 2018).

Photogrammetric flights

Six photogrammetric and one Lidar flights were used to observe diachronic evolution between 1956 and 2017 (Table 2). By means of the photogrammetric flights of 2001, 2005, 2010, 2014 and 2017 (Table 2) a photogrammetric restitution was made, except in the 1956 flight, and a 1/5000 scale map was drawn up following the General Process of Photogrammetry (Chris 2004). Ten terrain control points with coordinates obtained by GPS-RTK have given a planimetric mean square error $RMSE_{x,y} \leq 0.5$ m, and a altimetric mean square error $RSME_z \leq 1$ m (Soteres et al. 2011). The pixel size on the ground (GSD) was 0.22 cm and on the orthophotographies, 0.25 cm. The positional accuracy of the points is ± 20 mm, obtained in the ETRS89 coordinate system by means of a GPS-RTK (Leica 1200 GNSS). The 1/5000 cartographic scale has a planimetric tolerance of 1 m (0.2 mm for the denominator of the scale) and the equidistance of the contour lines is 2 m. The planimetric accuracy obtained by photogrammetric restitution are < 1 m and the altimetric accuracy are > 0.67 m.

Terrestrial laser scanner (TLS)

The use of TLS permits any changes and the extent of erosion to be estimated in detail. This technique has recently been applied in different coastal areas (Fabbri et al. 2017; Earlie et al. 2014; Sanjosé et al. 2018, 2020; Medjkane et al. 2018; Westoby et al. 2018; Xiong et al. 2019). Two annual measurements over a period of eight years (a total of 15 measurements) were made with TLS from May 2012 to March 2019 using six or seven scanning stations, depending on the year, to obtain 3D information of the coast before

and after winter storms. At least four common targets at each of four stations were used to join the 250 million points established for fieldwork. The DEMs were calculated and the difference between the successive point clouds and differences between surface models were later measured. In addition, nine profiles (P1–P9) were compared to quantify changes in the cliff, and profiles 1, 5, 8 and 9 are showed in Fig. 8. The application of TLS is fully efficient at detecting annual changes, working even under adverse meteorological conditions (Lindenbergh et al. 2011; Hoffmeister et al. 2012; Sanjosé et al. 2016, 2018). The scanner captures the 3D position of data points in the survey area, collecting the x , y , and z coordinates and the reflection intensity of each point (Kuhn and Prüfer 2014). A Leica ScanStation C10 scanner was used to calculate the positioning error of the targets with GNSS (± 20 mm) and the value of the $RMSE_{x,y,z} \leq 3$ cm. To calculate these parameters spatial determination (± 6 mm the uncertainty due to changes in the vegetation between shots or its movement by the wind during the measurement) was taken into consideration. The spatial point information of the resulting point cloud was used to derive accurate DEMs (Bremer and Sass 2012; Jaboyedoff et al. 2012).

Results

Morphodynamic features of the cliff and the beach

The Gerra Beach has a cliff of 45 m in height with varied slope gradients. The higher gradients are located in the Western and Eastern extremes on rock cliffs, with slopes gradients between 48° and 59° . In the central Eastern area the slopes are lower, between 30° and 43° , and the lowest gradients are located on the landslides, where slopes gradients around 20° have been measured. Under cliffs a beach system is developed. Three morphodynamic units can be differentiated (Fig. 3):

- (i) The upper platform; the old flat erosional surface, located at 40–50 m, where streams have carved out small hanging valleys over the cliff. Some small karstic features such as dolines and karstic depression are scattered over the surface of the calcareous rocks (Fig. 4, up).
- (ii) The coastal cliff; organized in three main sectors. The cliff-top is an irregular slope with visible substrate outcrop, from turbiditic at the East, to conglomerates and calcareous breccias in the center and claystone to the West. All slope processes are concentrated in the central part to form a vertical profile. The cliff is highly unstable, with small walls, active and inactive rockfalls and landslides. At the base, slope processes are induced by the wave action on soft rocks.

Table 2 Photogrammetric and lidar flights

| Flight | Institution | Calibration certificate | Characteristics |
|--------|-------------|-------------------------|---|
| 1956 | US Army | No | Orthophotography. Spanish national geographic institute (IGN) |
| 2001 | PNOA | Yes | |
| 2005 | PNOA | Yes | |
| 2010 | PNOA | Yes | |
| 2012 | PNOA | No | Light detection and ranging (LIDAR) |
| 2014 | PNOA | Yes | |
| 2017 | PNOA | Yes | |

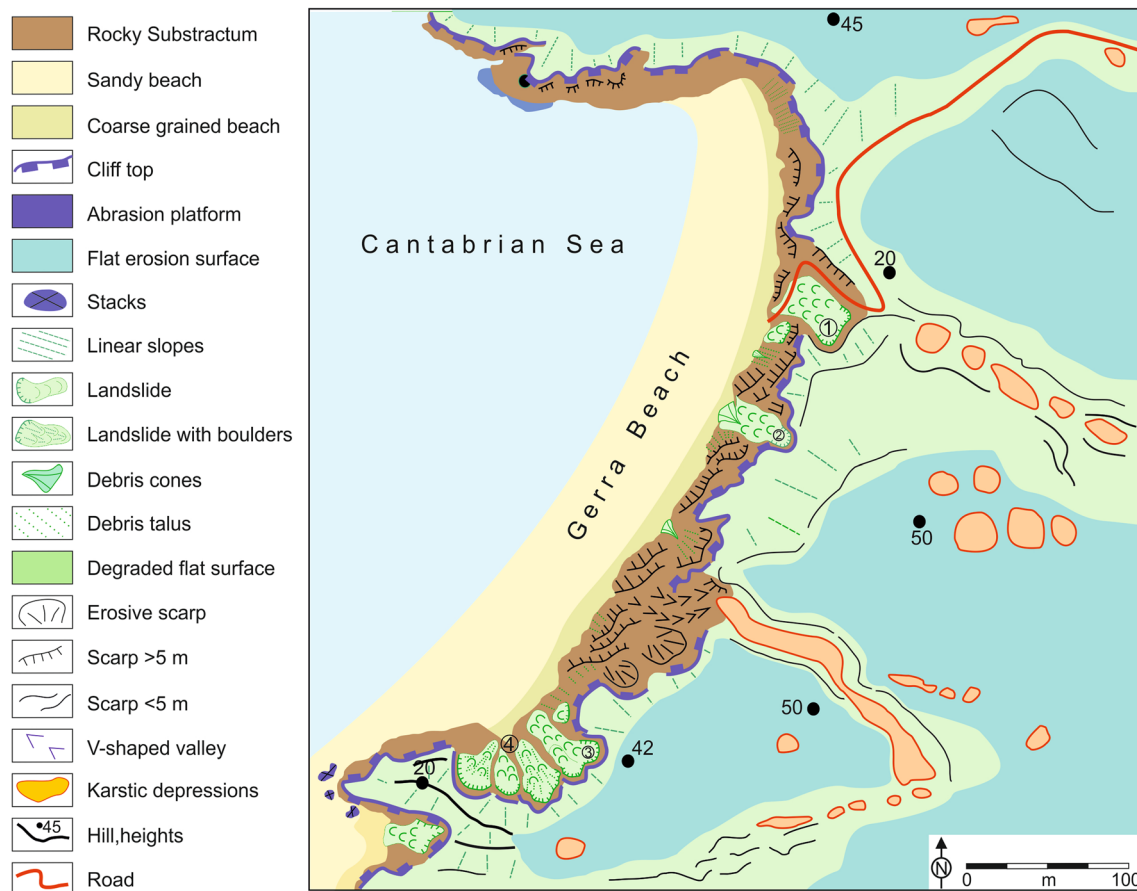


Fig. 3 Geomorphological sketch of Gerra Beach. The coarse grained beach includes the mixed sand and cobbles, boulder and sand, and scattered coarse grained beaches referred in the text. Circled numbers point the four landslides in Tables 3 and 5

Landslides and cracks are determined by geological structure and marine action due to the alternation of marls, sandstone and limestone, while the claystone outcrop determines the predominant processes, rockfalls or landslides, when the waves land on the substrate.

- Rockfalls. Small detachments (4–6 m wide) of turbidite formations of rock fragments mainly affect the cliff foot. Fine sediments with calcareous or sandstone blocks accumulate and arrange small talus and cones on the beach, burying the marine deposits. The fallen material can amount to around 20–30 m³/year, with the small talus and cones changing annually. Sometimes, isolated rock falls are channeled by gullies down to the beach. Several large blocks are scattered by the beach.
- Landslides. Between 2012 and 2019 the TLS measurements revealed four landslides on the cliff. On the turbidite formation in the East three translational or planar landslides have developed. There

are small portions of loam with breccias and calcareous blocks scattered by the cliff to form small debris flows, which only affect the turbidite formation.

The most active landslide (no 4 in Table 3 and Fig. 3) is in the Western sector. It is a complex or compound landslide generated on the Triassic claystone contact with the calcareous breccia and turbiditic sequence of limestone, marls and sandstones. The sliding process is produced by erosion on the cliff and claystone mass displacement downslope including turbidities and breccia. The arrangement zone is made up of at least five main scarps with coalescent crowns located at 41 m. The maximum width at the upper part of the landslide reaches approximately 54 m. On the transit and deposition area the displaced claystone, breccias, limestone and sandstone cover the outcrop of claystone. The main processes involved are landslides, rockfalls, and small rockflows (Figs. 3 and 5). At the shoreline, the displaced masses form heterometric and irregular deposits including

Fig. 4 Up, view of the Gerra Beach and San Vicente-Merón beaches system from the East and flat erosional surfaces (Rasas). Down, cliff of the Gerra Beach: 1, calcareous breccia. 2, claystone. 3, stratified limestone and marls

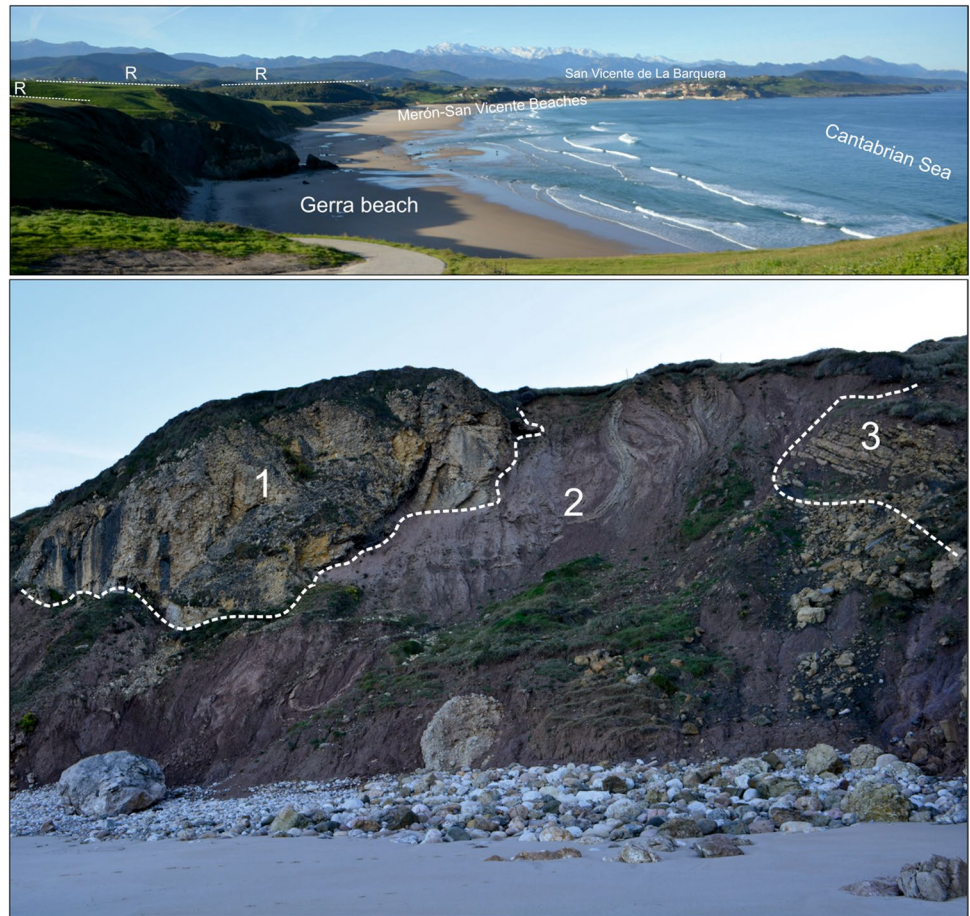


Table 3 Existing landslides in the Gerra sea cliff

| Slide no | Type ^a | Length (m) | Wide (m) | Altitude m a.s.l | | Surface (m ²) |
|----------|-------------------------|------------|----------|------------------|-----|---------------------------|
| | | | | Max | Min | |
| 1 | Translational or planar | 43 | 20 | 26 | 7 | 957 |
| 2 | Translational or planar | 22 | 12 | 25 | 7 | 250 |
| 3 | Translational or planar | 32 | 11/21 | 34 | 6 | 422 |
| 4 | Complex or compound | 41 | 54 | 38 | 8 | 1480 |

^aClassification according to Dikau et al. (1996) and Hungr et al. (2014)

breccia boulders larger than 2 m. The deposits, eroded by wave action, have a rectilinear limit.

The beach under the cliff (no. 4 in Fig. 6); located in the intertidal area, the profile of the beach changes seasonally with sand feeding and dragging, and some stacks are scattered by the beach. All beaches analyzed in this paragraph are included as coarse grained beach in Fig. 3. It is a composite beach (Jennings and Shulmeister 2002), in which four geomorphic environments can be differentiated (Fig. 6, Table 4):

- Abrupt slope change and talus. A slope change on the rocky substrate is continuous along the cliff and is

located at around 8–10 m height. It is constant throughout the cliff portion, only interrupted by seasonal rock fall. The slope accumulations formed by fines (loam, clays and sand) and boulder (limestone and sandstone) come from the wall and are reworked by wave action and newly transported onto the cliff. Boulder size ranges between 40–15 cm, and 5–10 cm.

- Mixed sand, pebbles and cobble beaches at the cliff-foot (no. 4 in Fig. 6). A beach deposit consisting of high proportions of both coarse particles, cobbles mainly, and fines. Away from the cliff at between 10 and 15 m, this is a narrow band with a slope of 30° located in the supratidal area as a storm berm. The fine-supported

Fig. 5 Geomorphological features of Gerra cliff (2018).

A Eastern side: 1, sand beach. 2, boulder beach. 3, cliff. 4, landslide. 5, rockfall. 6, flat erosional surface. **B** Rockfall. 1, boulder accumulation on the storm berm. **C** Landslide in the Western side of Gerra beach: 1, sand beach. 2, boulder beach. 3, planar slide. 4, rockfall. **D** Planar slide detail in the Western side of Gerra Beach: 1, sand beach. 2, boulder beach. 3, slide main body. 4, main scarp on claystone



structure is defined by a 30% fine texture. Clasts have a planar fabric (94%), clast size between 4 and 9 cm represent the 68% and boulders the 30%. Clasts are rounded (92%) and low sphericity is dominant (78%), although angular (4%) and uneven (6%) clasts come from the cliff (Fig. 6).

- Boulder beach (no. 3 in Fig. 6). A band of 8–10 m in length is characterized by a pebble, cobble and boulder beach with a 20° slope. The main block size is between 4 and 9 cm, with clasts up to 40 cm and scattered blocks of 3 m. The formation has a clast-supported structure, imbricate fabric and highly heterometric clasts. The clasts are rounded (100%) and dominate the low sphericity clasts, although the rounded and uneven ones make up 30% of the clasts measured. The larger scattered boulders are little worked by the sea, while the small-sized clasts are all rounded and wave reworked. The deposit is formed by clasts of limestone, sandstone and conglomerate. The clasts come from the cliff and are reworked by the wave action. The coarse-grained beach is located in the supratidal area, which is only occupied by the sea during the spring tides and storms.
- Sand and scattered coarse-grained beach (no 2 in Fig. 6). Away from the cliff in the intertidal area between 10 and 15 m, there is a narrow band of cobbles and sand with a 10–15° slope. The fine-supported structure is defined by a 40% sandy texture and clast with a planar fabric (73%). The main clast size is homometric and between 4 and 9 cm (80%). The deposit does not contain large boulders and clasts have a rounded morphology (76%) and low sphericity (Fig. 6, Table 4). The main rocks on the beach are limestone, sandstone and conglomerate and come from the cliff.
- Sand beach (no 1 in Fig. 6). Around 20 m from the cliff, the beach consists almost entirely of sand, located in the intertidal area, and only some calcareous stacks are located on the West side. Sand comes from the cliff and from the West. The dominant drift is from the NW and W, and the input of fine materials by the San Vicente estuary moves from West to East along the El Rosal, Merón and Bederna beaches before reaching the Eastern side of the beach system in Gerra Beach.

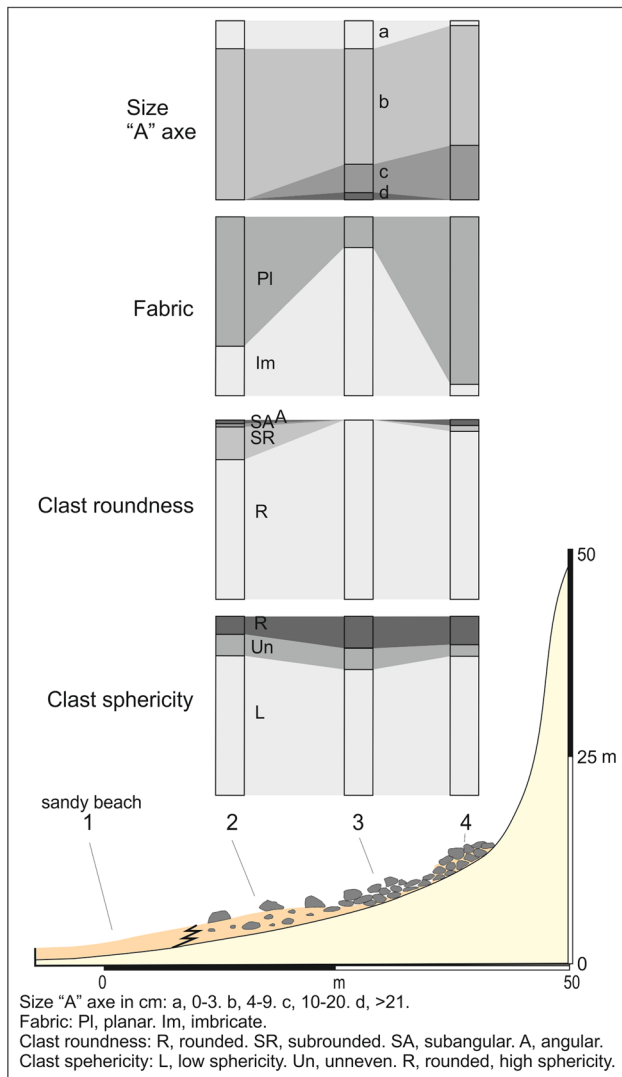


Fig. 6 Sedimentological data of Gerra Beach profile. 1, sandy beach. 2, mixed sand and cobble beach. 3, pure coarse-grained beach. 4, mixed sand and cobble deposits, storm berm. 5, landslide, boulder, gravel and fines—clays, silt and sand

Geomorphic dynamic and sediment distribution of the Gerra cliff

The main processes involved in the cliff erosion are landslides, in which large portions are removed during storm events by erosion at the base of the cliff. In the winter 2018–2019 on Gerra Beach, the Westernmost landslides were modified by a large rockfall and the landslide was partially covered by boulders. At same time, a new landslide was generated in the central part of the cliff. Rock outcrops on the cliff determine the distribution of landslides and rockfall. Claystone favors landslides, while on the turbidite outcrops rockfall are dominant.

The beach shows a decrease in clast sizes from the storm berm towards the sandy beach, but the coarse-grained beach has the greatest quantity of large blocks and the highest percentile. Also, cobbles and pebbles (< 10 cm) decrease towards the beach. The fabric is planar in the storm berm, and changes to imbricate in the coarse-grained beach, showing constant and high energy. All units have rounded clasts, although the greatest presence of subangular and angular clasts, from the cliff, is located in the backshore and storm berm. All of this points to the input of fine sediments, sands and gravels, and clasts from the cliff, and the input of fines sediments and smaller clasts to the foreshore. The boulder beach has very well sorted sediments and clasts well-rounded by the continuous wave energy during ordinary events.

In the sedimentary deposits of the cliff-foot the liquid limit is 36, the plastic limit (PL) 24, the plasticity index, 12, and the liquidity index -0.837 . The deposit is formed by low plasticity red claystone with a very low plasticity index. The material deformation can thus occur due to rainwater or wave spray, and not necessarily wave-pounding.

The grain size of the cliff-foot deposits is sand-silty (44% coarse sand, 40% fine sand and 16% silt and clay). The grain size of the sand beach is very well sorted (sandy, 90% fine sand and 10% coarse sand), but the fines of the boulder beach are moderately well sorted. The grain size shows the different action of transport processes. On the beach the competence of the transport process is moderate but very selective, generated by marine action; while in cliff-foot sediments the main process is the fall and flow from the rock outcrop, without secondary processes.

Sediments show a wave action affecting all areas of the beach, but there is a different dynamic between the boulder beach and the sand beach. If, at the cliff-foot and on the boulder beach the fines and angular clasts come from the cliff, on the beach the drift also join in, implying a better particles classification. The grain size distribution shows a rapid decrease from the cliff-foot to the sand beach, although the clasts on the boulder beach reach 4–9 cm in size. Grain size and roundness prove the cliff to be the origin of clasts. The substrate features (claystone, turbidites), therefore, determine the grain size of the beach since the main input consists of fines and small clasts. The highest wave energy focusses on the boulder beach, as proved by grain size, fabric and roundness (Table 4). These works as an energy sink and defend the cliff-foot.

Diachronic evolution of the coast through photogrammetric information (1956–2017)

The cartography obtained by photogrammetric methods between 2001 and 2017 do not show altimetric changes nor a significant retreat of the cliff-foot. Nevertheless,

Table 4 Grain size, clasts morphology and fabric of the Gerra Beach

| | 1 Sandy beach | 2 Coarse-grained beach | 3 Boulder beach | 4 Mixed blocky and sandy beach |
|------------------------------|------------------|---------------------------|--------------------|-----------------------------------|
| Clast size "L" axe. % | | | | |
| 0–3 cm | – | 16 | 16 | 2 |
| 4–9 cm | – | 84 | 64 | 68 |
| 10–20 cm | – | – | 18 | 30 |
| 21–34 cm | – | – | 1 | – |
| > 35 cm | – | – | 1 | – |
| Mean | – | 5 | 6.7 | 7.8 |
| SD | – | 0.63 | 2.79 | 4.83 |
| Centile cm | – | 12 | 55–300 | 16 |
| Fabric % | | | | |
| Imbricate | – | 27 | 83 | 6 |
| Planar | – | 73 | 17 | 94 |
| Clast roundness % | | | | |
| Rounded | – | 76 | 100 | 92 |
| Subrounded | – | 18 | – | 4 |
| Subangular | – | 3 | – | – |
| Angular | – | 3 | – | 4 |
| Clast sphericity % | | | | |
| Planar | – | 78 | 70 | 78 |
| Uneven | – | 12 | 12 | 6 |
| Round | – | 10 | 18 | 16 |
| Texture % | | | | |
| Fines | 100 | 40 | – | 30 |
| Clastic | – | 60 | 100 | 70 |
| Sands. grain size parameters | | | | |
| Mean μm | 290/335 | 350/480 | – | 310/520 |
| Sorting ϕ_1 | Mod. well sorted | Mod. sorted | – | Poorly sorted |
| Sk_1 | Positive | Negative | – | Negative |
| K_G | Leptokurtic | Platikurtic | – | Mesokurtic |
| Histogram | Unimodal | Polimodal | – | Bimodal |

larger retreats are detected in the cliff-top. The comparison of photogrammetric flights shows that the retreat in the coastline has been continuous since records began. During this period a large retreat has taken place in the Southern part of the beach (Fig. 7), where the greatest slippage takes place. The areas of the coastline with the smallest retreat between 1956 and 2001 are the most affected between 2001 and 2017 (16 years), with mean values of retreat of 20 m over 45 years (Fig. 7). In total, between 1956 and 2017 the maximum retreat in the coastline at the cliff-top is 42 m and the mean retreat 25 m.

In the whole cliff, the retreat was greater in the places where landslides were generated. Between 1956 and 2017, the mean retreat by landslide was 46 cm a^{-1} . For shorter periods highly active phases (2014–2017) of $200\text{--}300 \text{ cm a}^{-1}$ alternate with less dynamic ones (1957–2001), which

show retreat rates of between 0 and 150 cm a^{-1} , since each landslide event has a different behavior. Landslide 1 (see Fig. 3) is highly active over the long term but is revitalized from 2014 and produces a retreat in the cliff-face of between 200 and 300 cm a^{-1} . Previously it showed retreats of $30\text{--}46 \text{ cm a}^{-1}$, with a mean of 50 cm a^{-1} . Nevertheless, the retreat of landslide 2, which has shown the largest retreat in the period studied, reduces as we approach the present, reaching much reduced dynamism between 2014 and 2017.

The cliff faces show significantly lower retreat rates of between 20 and 100 cm a^{-1} . Retreat rates diminish from South to North and in all periods analyzed. Only in profile C a higher rate of retreat has been found in the most recent period. In the three profiles, a temporary increasing trend is seen in cliff retreat rates with a clear acceleration in the three profiles after 2014 (Table 5).

Fig. 7 Cliff-top evolution changes between 1956 and 2017. The contour lines correspond to 2017

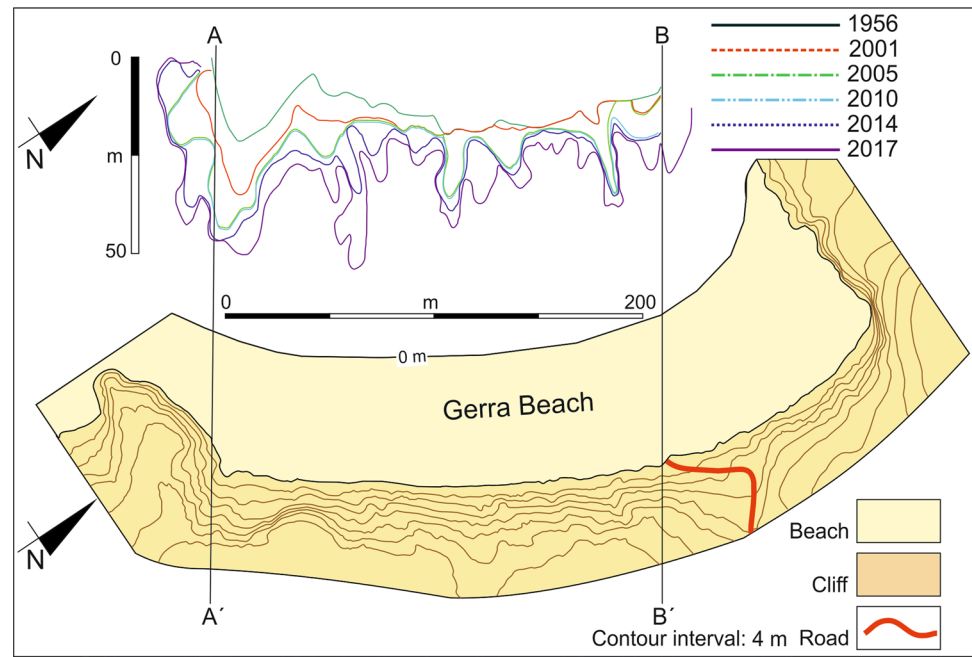


Table 5 Annual mean retreats

| Processes | | 1957–2017 (cm yr ⁻¹) | 1957–2001 (cm yr ⁻¹) | 2001–2014 (cm yr ⁻¹) | 2014–2017 (cm yr ⁻¹) | 2001–2017 (cm yr ⁻¹) |
|-----------|----|-------------------------------------|-------------------------------------|-------------------------------------|-------------------------------------|-------------------------------------|
| Type | No | | | | | |
| Landslide | 1 | 50 | 30 | 46 | 200 | 43.7 |
| | 2 | 70 | 150 | 123 | 5.5 | 200 |
| | 3 | 33.3 | 0 | 107.5 | 2 | 125 |
| | 4 | 30/34* | 40 | 30 | < 33 | < 0.3 |
| Cliff | A | 33.3 | 20 | 61.5 | 100 | 68.5 |
| | B | 11.5 | 10 | 15.5 | 33 | 18.7 |
| | C | 6.5 | 1.25 | 3.8 | 83.5 | < 6.6 |

* Measured until the year 2014, when the landslide come inactive

Terrestrial laser scanner (2012–2019)

In the spring and autumn DEMs nine cliff and beach profiles have been carried out perpendicular to the coastline and 25 m apart (Fig. 8). Profile 5 showed slippage in March 2018 and profile 8 was more stable except at the cliff-foot (Fig. 8). The most significant changes took place in the area affected by the wave-action, between 3 and 8 m above sea level, and where the material from rockfalls and landslides was carried and re-worked by the wave action. Changes happened from centimetric to metric scale, but the cliff foot was highly stable, unlike other parts of the Cantabrian Coast where storms were more efficient and damaging. The four large storms of 2013 are not reflected in morphological changes in the measurements of November 2013 or April 2014, and in any case are much smaller than those of other beaches in the Cantabrian Sea (Flor et al. 2014; Sanjosé et al. 2018).

The DEMs show the volumetric changes (Figs. 9 and 10) in the beach and the periods of accumulation and export of sediments. The altimetry of the beach varies between 0 and ±0.5 m, although there are differences of ±0.5–±1 m, and on occasion > 1 m. From spring 2012 until November 2019 399.66 m³ of sediments were accumulated on the beach and at the cliff-foot. This very small accumulation reveals the stability of the beach in spite of the great interannual variations. While between the spring of 2016 and the autumn of 2016 there was a gain of 3467.39 m³, between autumn and spring of 2016 the loss was of -3040.04 m³. A loss of material is appreciated during the winter cycles, but the summer cycle accumulation processes compensate the sand loss and balances the relationship between sediment gain and loss in periods between 1 and 4 years.

At the cliff, the DEMs show the re-activation by storms of some landslides during autumn 2013 and spring 2014, and between autumn 2017 and spring 2018 large mass

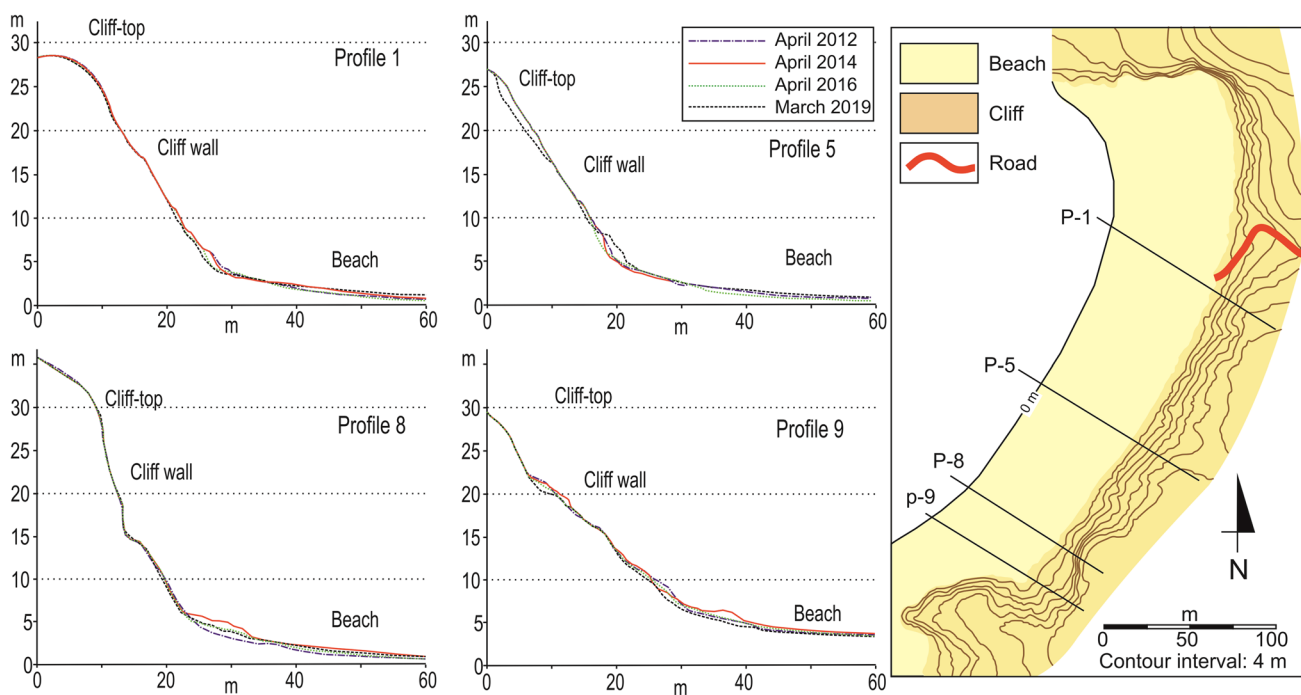


Fig. 8 Cliff evolution of profiles P1, P5, P8 and P9 made by TLS between 2012 and 2019. Profile 5 shows a landslide occurred in March 2018

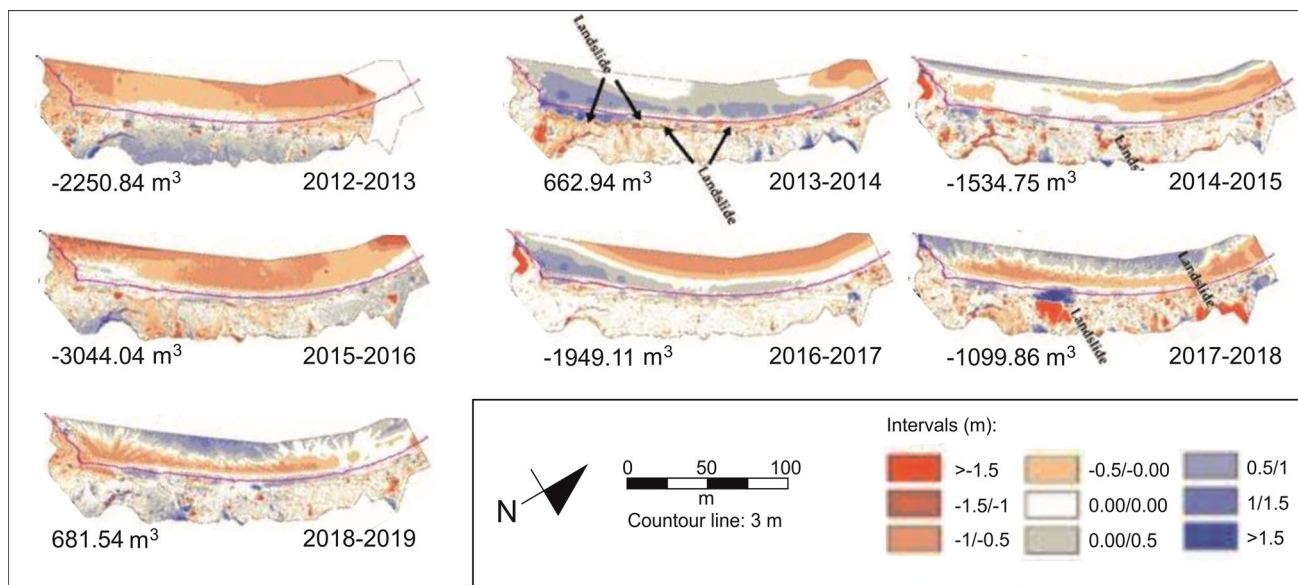


Fig. 9 Autumn–spring volumetric changes on the Gerra cliff from 2012 to 2019

movements also take place, which remained fully active in autumn 2019.

The loss of material between 2012 and 2019 between the foot and the head of the cliff-head amounted to -3633.32 m^3 , whereas the accumulation on the beach was 399.66 m^3 . Figures 9 and 10 denote the export of 3233.3 m^3 of sediments and an average of $404.2 \text{ m}^3 \text{ a}^{-1}$ of material that is washed out of the cove. As the sediments exported consist of fine

sands and clays, around $40 \text{ m}^3 \text{ a}^{-1}$ are transported afloat and the remaining $360 \text{ m}^3 \text{ a}^{-1}$ are carried by the currents. Although the most common drift is towards the East, the sedimentary cycle and the direction of sediment flow are not known. As the quantity of sand exported annually is very moderate and seasonal variations in the sand bank are far greater than these volumes, the stability of the beach is confirmed (Table 6).

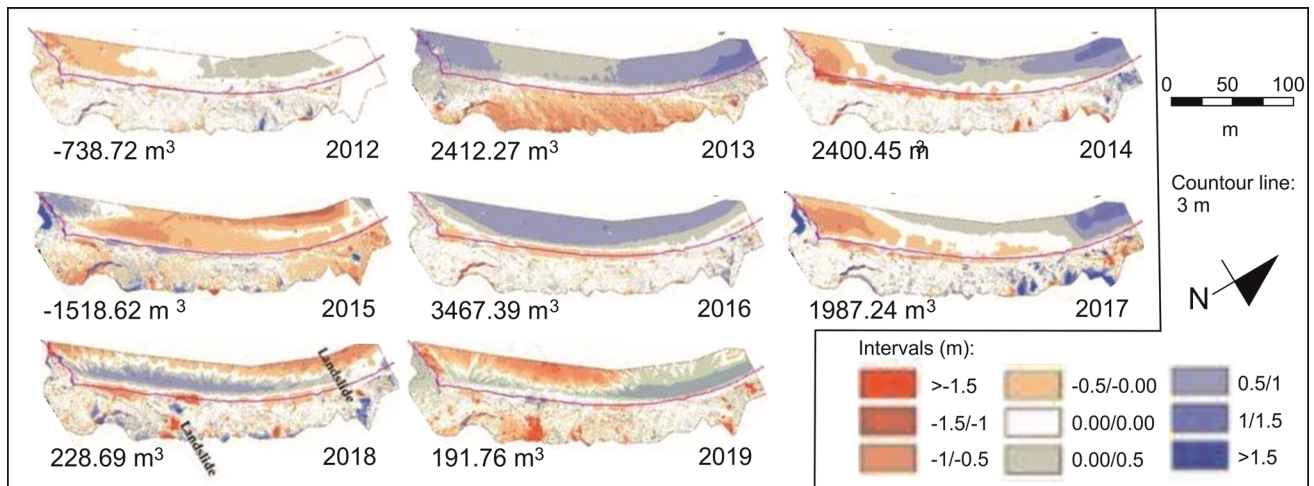


Fig. 10 Spring–autumn volumetric changes on the Gerra cliff from 2012 to 2019

Table 6 Annual volumetric changes in the Gerra Beach (2012–2019)

| Period* | Changes (m ³) | Balance (m ³) |
|-----------|---------------------------|---------------------------|
| 2012–2013 | –3289.56 | –214 |
| 2013–2014 | 3075.21 | |
| 2014–2015 | 865.70 | –1054.51 |
| 2015–2016 | –4562.66 | |
| 2016–2017 | 1518.28 | |
| 2017–2018 | 887.88 | |
| 2018–2019 | 910.23 | |
| Total** | –598.92 | |

*Annual cycles from spring to spring

**Total loss during the measured period

Discussion

It is well known that rock coast evolution and cliff erosion with subsequent deposition of large blocks is driven by large storms (Hansom 2001; Hall et al. 2008). In the Gerra Beach the turbidite and claystone lithostratigraphic units are hit by the waves during storm events that overlap with the high tide, but the ordinary action of the sea reworks and reshapes sediments and beach landforms throughout the year. During wave periods without storms the coarse-grained beach and deposits of the storm berm protect the cliff foot and there is no erosion.

Two event types characterize the beach dynamic. The first are high magnitude and low frequency events, or extreme ones, when the action of waves works on cliff-foot and berm deposits. It is mainly during storm events that erosion processes take place and berms are formed. Slope deposits fall on the storm berm and coarse-grained beach deposits are pushed and raised, which extracts fine

sediments from the cliff. These events work mainly during the autumn when high tides and storms take place, and winter. The cliff and highest part of the beach are modified by extraordinary events and swift changes take place. The second type of event is the high frequency and low energy events, or ordinary ones, when the constant action of waves on the coarse-grained beach export fines and small clasts. The coarse-grained beaches have the largest clast-size heterometry, fed by pebbles and blocks from the cliff during extraordinary events. Two differentiated beach units located on the backshore dissipate wave energy during ordinary events. The seasonal dynamic, with sand accumulations and output, implies less reworking of clasts and greater sorting of particles, from sand on the beach to an increase in blocks towards the cliff.

The period 2000–2014 was characterized by its many storms (Table 1), that did not give rise to significant changes to the cliff-foot line, but they did affect the cliff-top and mass movements in the slope. Measurements following the storms of March 2014 and later years (2015–2019) show a clear increase in mass movements. In this way the cliff-foot line remained stable, but the cliff-top line was modified by changes in root of the landslide (Fig. 11A).

The low plasticity of the rocks and deposits at the cliff-foot leads to the conclusion that wetting and wave action tend to generate rockfall and the accumulation of clasts on the beach. Nevertheless, the four landslides in the cliff are responsible for the greatest retreats of the cliff-top. These landslides were generated before 1957 in one case, between 1957 and 2001 in another, between 2001 and 2005 in a third case, with the last between 2005 and 2010. Active landslides are between more than 12 and 50 years old. On the volumetric maps re-activations and alternation of periods of erosion and accumulation can be observed (Figs. 9 and 10).

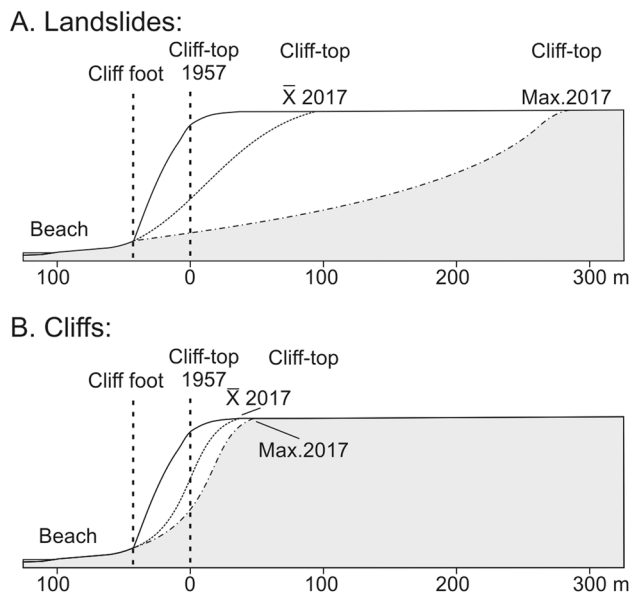


Fig. 11 Regression model in the Cliff of Gerra Beach during the last 60 years

The timing of the retreat is high and similar to those estimated for the European Atlantic coast and North Sea. On the South coast of England rates between 22 and 32 cm^{-1} have been estimated since 1870, and a recent acceleration has been observed (Hurst et al. 2016). In Brittany rates of around 45 cm a^{-1} (23–60 cm a^{-1}) were measured between the eighteenth century and 2016, but over a shorter period (1947–2016) the retreat is lesser at around 2–15 cm a^{-1} (Roulland et al. 2022). In the North Sea the recorded annual rates are 0.6 cm a^{-1} , however, for longer periods these rates increase to 20 and 60 cm a^{-1} (Westoby et al. 2018). In turbidite formations in Auckland retreat rates of between 2 and 198 cm a^{-1} have been measured (Moon and Healy 1994; Lange and Moon 2005) and a recent acceleration on the Eastern Mediterranean coast has also been detected, where the maximum retreat rate was 8 cm a^{-1} between 2006 and 2015 (Mushkin et al. 2018). The timing of cliff degradation in Gerra is similar to that of the Atlantic coast and North Sea, except in the case of Brittany in recent times.

Several authors have pointed to a recent acceleration of retreat rates of cliffs due to the combination of the increase in storms, sea level rise and human involvement (Trenhaile 2014; Hurst et al. 2016; Mushkin et al. 2018). The increase in storms is one of the determining factors in coastal evolution and recent changes (Trenhaile 2014; French and Burningham 2013; Hurst et al. 2016; Sanjosé et al. 2018). Nevertheless, in Gerra Beach, although we have not data previous to the twenty-first century, it may be that storms are not the most meaningful factor, unlike on other parts of the Cantabrian Coast (Flor et al. 2014; Sanjosé et al. 2018).

In Gerra Beach, direct human action does not involve the modification of the beach. The seaport facilities 3 km to the West mean an input of sediments from the seaport and the San Vicente Estuary. The loss of sediment during the study period indicates that the input of sediments from the estuary is not very great, even though the San Vicente beach system is linked to the estuary. Among the factors that point to potential increases in the retreat of the cliffs, such as the increase in rainfall and extraordinary rainfall events, the increase in storms and the impact of waves due to the rise in sea level (Trenhaile 2014), only the latter may explain a potential increase retreat rates at Gerra Beach. Therefore, an increase in the processes of erosion and the output of sediments related to the global sea-level rise and the more frequent rise in storm waves reaching the cliff foot can be expected.

The retreat of the cliff-top is not continuous. A greater rate of retreat has been detected where landslides are generated (Table 5), and as the recent TLS measurements show it fits the alternation of periods with high rates of retreat and longer periods of equilibrium. Two important facts regarding cliff faces on other coasts have been mentioned. On one hand the succession of cycles with large collapses and retreats in the headland of the cliffs, which are of up to 15 m in each episode. On the other hand, periods with highly variable retreats along the coastline are in accordance with changes in the geological structure, rock types and mass movements taking place in the cliff (Moon and Healy 1994; Mushkin et al. 2018; Westoby et al. 2018). Therefore, we interpret that the rhythms of retreat detected take place in impulses with long periods of balance alternating with sudden collapses and with spatial variations throughout the cliff both in landslides and rockfalls. In cliff-faces the rates of retreat are lesser, clearly below the rates estimated and measured in the Mediterranean, North Sea and Atlantic (Hurst et al. 2016; Mushkin et al. 2018; Westoby et al. 2018). The profiles generated from the DEMs of the TLS do not point to changes in the cliff-foot except in the extreme situations of storms that modify it through small rockfalls, such as those of autumn 2013 and spring 2014. Nevertheless, the same DEMs show changes in the cliff top with greater landslides, like those of autumn 2017 and spring 2018. The storms of winter 2013 were the most aggressive of the twenty-first century (Table 2), on the Cantabrian Coast (Sanjosé et al. 2016, 2018; Garmendia et al. 2017; Rasilla et al. 2018), but the mark they left on the beach of Gerra was far lesser than that of other beaches along the same coastline.

The measurements of retreat permit an empirical model of cliff degradation to be established based on the high rates of change in the cliff-top and the stability of the cliff-foot. Unlike the more common processes in rock cliffs, with undercutting erosion by waves generating rock falls and the supply of coarse sediments, in Gerra the cliff top retreats

(Fig. 11B). Thus, the main retreat does not take place at the contact between the cliff and the beach, but that there is a degradation and gradual disappearance of the cliffs from the cliff-tops. The retreat, as is common to all cliffs (Moon and Healy 1994; Trenhaile 2014), is not linear and at the cliff-top the differences are of the order of 20–40 m. The boulder beach is of fundamental importance to dissipating wave energy (Earlie et al. 2014), such that both the fall in the effectiveness of the wave and the weakness of the clays favour landslides. In Gerra the geometry of the beach dissipates the energy from the waves at the access to the inlet, and at the same time the boulder beach weakens the wave action, except in extraordinary events at high tide. For Earlie et al. (2014) the retreat rhythms are related to the height of the wave and the rock strength. In Gerra the placement at the edge of the diapiric structure made up of strongly deformed clay, marl and limestone strata. So, the high rates of retreat at the cliff-top are facilitated by the rock type and structure. The progressive reduction of the cliff slope is mainly controlled by mass movements. But the increase in erosion, given the present day lower energy of the shore break and the absence of anthropic influence, leads to the consideration that the potential sea level rise and the erosion on the landslide fronts may be in the future the most important factor in the erosion of the cliff.

The photogrammetric flights reveal the continuous retreat of the coastline. We have not detailed data of the twentieth century, and only long period results can be interpreted, but in the twenty-first century this has been more accentuated than in the second half of the twentieth century, which agree with the recent acceleration detected in other coasts around the world (Cazenave and Le Cozannet 2013; Hurst et al. 2016; Mushkin et al. 2018). Regional projections indicate a rise in the sea level of around 10 cm in the North of Spain (Cazenave and Cozannet 2013), such that it takes on greater importance for the management of future risks to cliffs without direct anthropic intervention in Gerra and the Cantabrian Coast.

Conclusions

The combination of geomorphological, geomatic and sedimentological techniques is an effective tool for the detailed and local scale study of the dynamic of marine cliffs and their evolution. The combination of linear and volumetric changes together with the estimation of dominant processes in different parts of the cliff have provided knowledge on the evolution of the cliff as a whole over the last 65 years.

This study has facilitated the estimation of places, processes, in this case, landslides and the rockfalls, and the rates of degradation of the cliffs, all determined by the geological structure—strata dipping, diapir—and types of rocks. The

geomorphological trend of the cliff has been established as a process of degradation from the cliff-top to the cliff-foot, whereas the beach remains stable and the cliff-top back away in spite of the increase in storm events recorded on the Cantabrian Coast. The assessment of profiles clearly indicate that this beach is virtually stable, with no significant changes in the coast line because the beach is very effective in protecting the cliff-toe. So, only the rates increase of the sea level rise can change the retreat rhythms, accelerating the erosion of landslide fronts, the present day more active processes. The scarce influence of anthropic action and the mitigation of the wave action from storms in the Gerra cove mean that the potential effect of the rise in the sea level can be the most efficient erosive and degrading potential process on the cliff-foot. Nevertheless, erosion is now centred on the retreat of the cliff top, which involves the degradation of the cliff in the absence of the retreat of the coastline. So, the potential natural risks are concentrated in this area, and in the loss of soil.

As a whole, the behaviour observed reveals the diversity of processes and responses in the Cantabrian Coast in the face of recent changes, storm events and the sea level rise. It is showed the need to carry out detailed analysis of the dynamic of the cliffs for the follow-up of changes and management of natural risks in the context of sea level rise and climate change.

Acknowledgements This work has been made possible thanks to funding granted by the Consejería de Economía, Ciencia y Agenda Digital (Junta de Extremadura, Spain), by the European Regional Development Fund (European Union, reference grant GR21156), the PID2020-113247RBC21 project, of the Science and Innovation Spanish Ministry, and the Research Group on Natural Heritage and Applied Geography (GIR Pangea-University of Valladolid). The authors wish to dedicate this work as a grateful tribute to Prof. Augusto Pérez-Alberti, for his dedication and generosity to his colleagues, and for his important contributions to coastal and mountain geomorphology.

Author contributions All authors contributed to the study conception and design. Material preparation, data collection and analysis were performed by ES, JJS, MGL, MSF and AGG. The first draft of the manuscript was written by ES and JJS and all authors commented on previous versions of the manuscript. All authors read and approved the final manuscript

Funding Open Access funding provided thanks to the CRUE-CSIC agreement with Springer Nature.

Data availability Not applicable.

Declarations

Conflict of interest The authors declare no competing interests.

Open Access This article is licensed under a Creative Commons Attribution 4.0 International License, which permits use, sharing, adaptation, distribution and reproduction in any medium or format, as long as you give appropriate credit to the original author(s) and the source, provide a link to the Creative Commons licence, and indicate if changes were made. The images or other third party material in this article are included in the article's Creative Commons licence, unless indicated otherwise in a credit line to the material. If material is not included in the article's Creative Commons licence and your intended use is not permitted by statutory regulation or exceeds the permitted use, you will need to obtain permission directly from the copyright holder. To view a copy of this licence, visit <http://creativecommons.org/licenses/by/4.0/>.

References

- Benumof BT, Griggs GB (1999) The dependence of Seacliff erosion rates on cliff material properties and physical processes: San Diego County California. *Shore Beach* 7:29–41
- Blott SJ, Pye K (2001) GRADISTAT: a grain size distribution and statistics package for the analysis of unconsolidated sediments. *Earth Surf Proc Land* 26(11):1237–1248
- Bremer M, Sass O (2012) Combining airborne and terrestrial laser scanning for quantifying erosion and deposition by a debris flow event. *Geomorphology* 138:49–60. <https://doi.org/10.1016/j.geomorph.2011.08.024>
- Brunsdon D (2002) Geomorphological roulette for engineers and planners: some insights into an old game. *Q J Eng Geol Hydrogeol* 35:101–142
- Brunsdon D, Lee EM (2004) Behaviour of coastal landslide systems: an interdisciplinary view. *Zeitschr Geomorphol Suppl* 134:1–112
- Bruschi V, Remondo J (2019) The Cantabrian rocky coast. In: Morales JA (ed) *The Spanish coastal systems dynamic processes sediments and management*. Springer Verlag, Monach, pp 79–91
- Burden A, Smeaton C, Angus S, Garbutt A, Jones L, Lewis HD, Rees SM (2020) Impacts of climate change on coastal habitats relevant to the coastal and marine environment around the UK. *MCCIP Sci Rev*. <https://doi.org/10.14465/2020arc11chb>
- Cazenave A, Le Cozannet G (2013) Sea level rise and its coastal impacts. *Earth's Future* 2:15–34. <https://doi.org/10.1002/2013EF000188>
- Chris J (2004) *Manual of photogrammetry*. American Society for Photogrammetry and Remote Sensing, Maryland
- Das BM (2006) *Principles of geotechnical engineering*. Thomson Learning College, Stamford
- de Lange W, Moon VG (2005) Estimating long-term cliff recession rates from shore platform widths. *Eng Geol* 80:292–301. <https://doi.org/10.1016/j.enggeo.2005.06.004>
- Dikau R, Brunsden D, Schrott L, Ibsen ML (1996) *Landslide recognition identification, movements, causes*. Wiley and Sons, New York
- Domínguez-Cuesta MJ, Jiménez-Sánchez M, González-Fernández JA, Quintana L, Flor G, Flor-Blanco G (2015) GIS as a tool to detect flat erosional surfaces in coastal areas: a case study in North Spain. *Geol Acta* 13:97–106. <https://doi.org/10.1344/GeologicaActa2015.13.2.2>
- Domínguez-Cuesta MJ, Gonzalez-Pumariega P, Valenzuela P, Lopez-Fernández C, Rodríguez-Rodríguez L, Ballesteros D, Mora M, Meléndez M, Herrera F, Marigil MA, Pando L, Cuervas-Mons J, Jiménez-Sánchez M (2022) Understanding the retreat of the Jurassic Cantabrian Coast (N. Spain): comprehensive monitoring and 4D evolution model of the Tazones Lighthouse landslide. *Mar Geol* 449:106836
- Dornbusch U, Robinson DA, Moses CA, Williams RBG (2008) Temporal and spatial variations of chalk cliff retreat in East Sussex 1873 to 2001. *Mar Geol* 249:271–282
- Earlie CS, Masselink G, Russell PE, Shail RK (2014) Application of airborne LiDAR to investigate rates of recession in rocky coast environments. *J Coast Conserv Plan Manage* 19(6):831–845. <https://doi.org/10.1007/s11852-014-0341>
- Fabbi S, Giambastiani BM, Sistilli F, Scarelli F, Gabbianelli G (2017) Geomorphological analysis and classification of foredune ridges based on Terrestrial Laser Scanning (TLS) technology. *Geomorphology* 295:436–451. <https://doi.org/10.1016/j.geomorph.2017.08.003>
- Flor G (1983) Las rasas asturianas. Ensayo de correlación y emplazamiento. *Trabajos Geol* 13:65–81. <https://doi.org/10.17811/tdg.13.1983.65-83>
- Flor G, Flor-Blanco G (2014) Raised beaches in the Cantabrian coast. In: Gutiérrez F, Gutiérrez M (eds) *Landscapes and landforms of Spain world geomorphological landscapes*. Springer Science, Dordrecht, pp 239–248
- Flor G, Flor-Blanco G, Flores-Soriano C (2014) Cambios ambientales por los temporales de invierno de 2014 en la costa asturiana (NO de España). *Trabajos Geol* 34:97–123. <https://doi.org/10.17811/tdg34201497-12>
- Flor-Blanco G, Pando L, Morales JA, Flor G (2015) Evolution of beach-dune fields systems following the construction of jetties in estuarine mouths (Cantabrian Coast NW Spain). *Environ Earth Sci* 73:1317–1330. <https://doi.org/10.1007/s12665-014-3485-1>
- Flor-Blanco G, Alcántara-Carrión J, Jackson DWT, Flor G, Flores-Soriano C (2021) Coastal erosion in NW Spain: recent patterns under extreme storm wave events. *Geomorphology* 387:107767. <https://doi.org/10.1016/j.geomorph.2021.107767>
- Flor-Blanco G, Bruschi V, Adrados L, Domínguez-Cuesta MJ, Gracia-Prieto FJ, Llana-Fúnez S, Flor G (2022) Geomorphological evolution of the calcareous coastal cliffs in North Iberia (Asturias and Cantabria regions). *Estuar Coast Shelf Sci* 273:107913. <https://doi.org/10.1016/j.jecss.2022.107913>
- Folk RL (1980) *Petrology of sedimentary rocks*. Hemphill, Austin
- French JR, Burningham H (2013) Coasts and climate: Insights from geomorphology. *Prog Phys Geogr* 37(4):550–561. <https://doi.org/10.1177/0309133313494962>
- Garmendia C, Rasilla DF, Rivas V (2017) Distribución espacial de los daños producidos por los temporales del invierno 2014 en la costa norte de España: Peligrosidad vulnerabilidad y exposición. *Estud Geogr*. <https://doi.org/10.3989/estgeogr201703>
- Garrote J, Garzón G, Page J (2001) Condicionamientos antrópicos en la erosión de la playa de Oyambre (Cantabria). *Actas V Reunión de Cuaternario Ibérico. Universidad de Oviedo, Oviedo*, pp 67–70
- Garrote J, Garzón-Heydt G, Alcántara-Carrión J (2002) Influencia de los temporales sobre el transporte de sedimentos en la Playa de Oyambre (Cantabria N de España). *Actas V Reunión Nacional de Geomorfología. Universidad de Valladolid, Valladolid*, pp 361–371
- Garrote J, Díaz-Álvarez A, Nganhane HV, Garzón-Heydt G (2018) The severe 2013–14 winter storms in the historical evolution of Cantabrian (Northern Spain) beach-dune systems. *Geosciences* 8:459. <https://doi.org/10.3390/geosciences8120459>
- Garzón-Heydt G, Alonso A, Torres T, Llamas J (1996) Edad de las playas colgadas y de las turberas de Oyambre y Meron (Cantabria). *Geogaceta* 20(2):498–501
- Gómez-Gutiérrez A, Goncalves GR (2020) Surveying coastal cliffs using two UAV platforms (multirotor and fixed-wing) and three different approaches for the estimation of volumetric changes. *Int*

- J Remote Sens 41(21):8143–8175. <https://doi.org/10.1080/0143161.2020.1752950>
- González-Amuchástegui MJ, Serrano E, Edeso JM, Meaza G (2005) Cambios del nivel del mar durante el Cuaternario y morfología litoral en la costa oriental cantábrica (País Vasco y Cantabria). In: Sanjaume E, Mateu J (eds) Geomorfología Litoral i Quaternari. Publicacions Universitat de Valencia, Valencia, pp 167–180
- Hall AM, Hansom JD, Jarvis J (2008) Patterns and rates of erosion produced by high energy wave processes on hard rock headlands: the grind of the Navir Shetland Scotland. *Mar Geol* 248:28–46. <https://doi.org/10.1016/j.margeo.2007.10.007>
- Hansom J (2001) Coastal sensitivity to environmental change: a view from the beach. *CATENA* 42:291–305. [https://doi.org/10.1016/S0341-8162\(00\)00142-9](https://doi.org/10.1016/S0341-8162(00)00142-9)
- Heredia N, Robador A, Rodríguez LR (1990) Cantabria. Mapa geológico-minero. ITGE-Diputación Regional de Cantabria, Madrid
- Hernández-Pacheco F, Asensio-Amor I (1966) Fisiografía y sedimentología de la playa y ría de San Vicente de La Barquera. *Estud Geol* 22:1–23
- Hoffmeister D, Tilly N, Curdt C, Aasen H, Ntageretzis K, Hadler H, Willershäuser T, Vött A, Bareth G (2012) Terrestrial laser scanning for coastal geomorphologic research in Western Greece. *Int Arch Photogram Remote Sens Spat Inf Sci* 39:511–516. <https://doi.org/10.5194/isprsarchives-XXXIX-B5-511-2012>
- Hungu O, Leroueil S, Picarelli L (2014) The Varnes classification of landslides types an update. *Landslides* 11:167–194. <https://doi.org/10.1007/s19346-013-0436-y>
- Hurst MD, Rood DH, Ellis MA, Anderson RS, Dornbusch U (2016) Recent acceleration in coastal cliff retreat rates on the South coast of Great Britain. *PNAS* 113(47):13336–13341. <https://doi.org/10.1073/pnas.1613044113>
- IGME (2009) Mapa geológico de España E 1/50000 Comillas No 33. IGME, Ministerio de Industria, Madrid
- Jaboyedoff M, Oppikofer T, Abellán A, Derron MH, Loye A, Metzger R, Pedrazzini A (2012) Use of LIDAR in landslide investigations: a review. *Nat Hazards* 61:5–28. <https://doi.org/10.1007/s11069-010-9634-2>
- Jennings R, Shulmeister JA (2002) Field based classification scheme for gravel beaches. *Mar Geol* 186:211–228. [https://doi.org/10.1016/S0025-3227\(02\)00314-6](https://doi.org/10.1016/S0025-3227(02)00314-6)
- Kuhn D, Prüfer S (2014) Coastal cliff monitoring and analysis of mass wasting processes with the application of terrestrial laser scanning: a case study of Rügen Germany. *Geomorphology* 213:153–165. <https://doi.org/10.1016/j.geomorph.2014.01.005>
- Letortu P, Costa S, Bensaid A, Cador JM, Quénoel H (2014) Vitesses et rythmes de recul des falaises crayeuses de Haute-Normandie (France): méthodologie et variabilité du recul. *Géomorphologie* 2:133–144
- Letortu P, Costa S, Cador JM, Coinaud C (2015a) Statistical and empirical analyses of the triggers of coastal chalk cliff failure. *Earth Surf Process Landform* 40(10):1371–1386. <https://doi.org/10.1002/esp.3741>
- Letortu P, Costa S, Maquaire O, Delacourt C, Augereau E, Davidson R, Suanez S, Nabucet J (2015b) Retreat rates modalities and agents responsible for erosion along the coastal chalk cliffs of Upper Normandy: the contribution of terrestrial laser scanning. *Geomorphology* 245:3–14. <https://doi.org/10.1016/j.geomorph.2015.05.007>
- Lindenbergh RC, Soudarissanane SS, Vries SD, Gorte BGH, Schipper MAD (2011) Aeolian beach sand transport monitored by terrestrial laser scanning. *Photogram Rec* 26:384–399. <https://doi.org/10.1111/j.1477-9730.2011.00659x>
- Lorenzo F, Alonso A, Pagés JL (2007) Erosion and accretion of beach and spit systems in North West Spain: a response to human activity. *J Coastal Res* 23:834–845
- Losada M, Medina R, Vidal C, Roldán A (1991) Historical evolution and morphological analysis of “el Puntal” spit Santander (Spain). *J Coastal Res* 7:711–722
- Marques FMSF (2006) Rates patterns timing and magnitude-frequency of cliff retreat phenomena. A case study on the West coast of Portugal. *Zeitschr Geomorphol Suppl* 144:231–257
- Medjkane M, Maquaire O, Costa S, Roulland T, Letortu P, Fauchard C, Antoine R, Davidson R (2018) High-resolution monitoring of complex coastal morphology changes: cross-efficiency of SfM and TLS-based survey (Vaches-Noires cliffs Normandy France). *Landslides* 15:1097–1108. <https://doi.org/10.1007/s10346-017-0942-4>
- Moñino M (1987) Variaciones del nivel del mar en la costa de Cantabria durante el Cuaternario. *Actas VIII Reunión Nacional de Cuaternario-AEQUA*. Universidad de Cantabria, Santander, pp 233–236
- Moon VG, Healy G (1994) Mechanisms of coastal cliff retreat and hazard zone delineation in soft flysch deposits. *J Coastal Res* 10(39):663–680
- Mushkin A, Katz O, Porat N (2018) Overestimation of short-term coastal cliff retreat rates in the Eastern Mediterranean resolved with a sediment budget approach. *Earth Surf Proc Land* 44:179–190. <https://doi.org/10.1002/esp.4490>
- Naylor LA, Stephenson WJ, Trenhaile AS (2010) Rock coast geomorphology: recent advances and future research directions. *Geomorphology* 114:3–11. <https://doi.org/10.1016/j.geomorph.2009.02.004>
- Nicholls RJ, Wong PP, Burkett VR, Codignotto JO, Hay JE, McLean RF, Ragoonaden S, Woodroffe CD (2007) Coastal systems and low-lying areas climate change 2007: impacts adaptation and vulnerability. In: Parry ML, Canziani JP et al (eds) Contribution of working group II to the fourth assessment report of the intergovernmental panel on climate change. Cambridge University Press, Cambridge, pp 315–356
- Olsen M, Johnstone E, Driscoll N, Ashford S, Kuester F (2009) Terrestrial laser scanning of extended cliff sections in dynamic environments: parameter analysis. *J Surv Eng* 135:161–169
- Pierre G, Lahousse P (2006) The role of groundwater in cliff instability: an example at Cape Blanc-Nez (Pas-de-Calais France). *Earth Surf Proc Land* 31:31–45. <https://doi.org/10.1002/esp.1229>
- Rasilla DF, García-Codrón JC, Garmendia C, Herrera S, Rivas V (2018) Extreme wave storms and atmospheric variability at the Spanish coast of the Bay of Biscay. *Atmosphere* 9:316. <https://doi.org/10.3390/atmos9080316>
- Rivas V, Cendrero A (1994) Human influence in a low-hazard coastal area: an approach to risk assessment and proposal of mitigation strategies. *J Coastal Res* 12:289–298
- Rosser NJ, Petley DN, Lim M, Dunning SA (2005) Terrestrial laser scanning for monitoring the process of hard rock coastal cliff erosion. *Q J Eng Geol Hydrogeol* 38:363–375
- Roulland T, Maquaire O, Costa S, Medjkane M, Davidson R, Fauchard C, Antoine R (2022) Seasonal activity quantification of coast badlands by TLS monitoring over five years at the “Vaches Noires” cliffs (Normandy France). *Geomorphology* 400:108083. <https://doi.org/10.1016/j.geomorph.2021.108083>
- Sanjosé JJ, Serrano E, Berenguer F, González-Trueba JJ, Gómez-Lende M, González-García M, Guerrero-Castro M (2016) Evolución histórica y actual de la línea de costa en la playa de Somo (Cantabria) mediante el empleo de la fotogrametría aérea y escáner láser terrestre. *Cuaternario Geomorfol* 30:119–130. <https://doi.org/10.17735/cygv.30i1-241464>
- Sanjosé JJ, Gómez-Lende M, Sánchez-Fernández M, Serrano E (2018) Monitoring retreat of coastal sandy systems using geomatics techniques: Somo Beach (Cantabrian Coast Spain 1875–2017). *Remote Sens* 10:1500. <https://doi.org/10.3390/rs10091500>
- Sanjosé JJ, Serrano E, Sánchez-Fernández M, Gómez-Lende M, Redweik P (2020) Application of multiple geomatic techniques for

- coastline retreat analysis: the case of Gerra Beach (Cantabrian Coast Spain). *Remote Sens* 12:3669. <https://doi.org/10.3390/rs12213669>
- Soteres C, Rodríguez AF, Martínez J, Ojeda JC, Romero E, Abad P (2011) Publicación de datos LiDAR mediante servicios web estándar. In: II Jornadas Ibéricas de Infraestructuras de Datos Espaciales, Consejo Superior Geográfico, Barcelona. <https://www.idee.es/resources/presentaciones/JIIDE11/Articulo-70.pdf>
- Trenhaile AS (2014) Climate change and its impact on rock coasts. *Geol Soc Lond Mem* 40:7–17. <https://doi.org/10.1144/M40.2>
- Trenhaile AS (2016) Rocky coasts. Their role as depositional environments. *Earth Sci Rev* 159:1–13
- Tucker M (1988) *Techniques in sedimentology*. Blackwell, Oxford
- Tucker ME (2001) *Sedimentary petrology*. Blackwell, Oxford
- Westoby MJ, Lim M, Hogg M, Pound MJ, Dunlop L, Woodward J (2018) Cost-effective erosion monitoring of coastal cliffs. *Coast Eng* 138:152–164. <https://doi.org/10.1016/j.coastaleng.201804008>
- Xiong L, Wang G, Bao Y, Zhou X, Wang K, Liu H, Sun X, Zhao R (2019) A rapid terrestrial laser scanning method for coastal erosion studies: a case study at Freeport Texas, USA. *Sensors* 19(15):3252. <https://doi.org/10.3390/s19153252>
- Young AP, Ashford SA (2006) Application of airborne LIDAR for seacliff volumetric change and beach sediment contributions. *J Coast Res* 22:307–318
- Young AP, Ashford SA (2008) Instability investigation of cantilevered seacliffs. *Earth Surf Proc Land* 33:1661–1677. <https://doi.org/10.1002/esp1636>
- Young AP, Flick RE, Gutierrez R, Guza RT (2009) Comparison of short-term seacliff retreat measurement methods in Del Mar California. *Geomorphology* 112:318–323. <https://doi.org/10.1016/j.geomorph.200906018>

Publisher's Note Springer Nature remains neutral with regard to jurisdictional claims in published maps and institutional affiliations.